**Review**

# Pyrotechnic Countermeasures: II. Advanced Aerial Infrared Countermeasures

**Ernst-Christian Koch***

Diehl BGT Defence GmbH & Co. KG, Fischbachstrasse 16, D-90552 Röthenbach a. d. Pegnitz, Germany

DOI: 10.1002/prep.200600001

**Abstract**

This paper discusses the technology of advanced aerial infrared countermeasures and related work disclosed in the unclassified literature. Missile-seeker head counter-countermeasures include spectral discrimination, kinematical discrimination, rise-time discrimination, UV/VIS discrimination and area temperature matching. Advanced flare payloads designed to counter dual color seekers contain selectively emitting compositions based primarily on high carbon fuels and perchlorates. Other advanced payloads consist of low temperature emitters like pyrophoric metal foils and gasless pyrotechnic compositions like Fe/$KClO_4$. The optimization of black body flares, still considered essential to a successful countermeasure solution, make use of new fuels based on e.g. meta-stable alloys and nanometer-sized powders as well as high energetic oxidizers. Kinematic flares today use combined propellant and infrared grains. 116 references from the public domain are given. For part I see Ref. [1].

**Keywords:** Advanced Flare Compositions, Decoy Flares, Pyrotechnics, Pyrophorics

## 1 Introduction and Scope of Work

Recently the author has discussed the general function and technology of aerial infrared decoy flares to counter infrared-guided Surface-to-Air (SAM) and Air-to-Air (AAM) missiles [1]. Since then there has been a substantial growth on publications devoted to advanced flare materials and technology. In addition the "infrared threat" has substantially changed since 09-11-2001, so today civil airliners are also potential targets of infrared guided missiles and must be protected adequately [2]. Hence it is the purpose of the present paper to provide an overview on advanced expendable infrared countermeasure technology disclosed in the open literature.

When dealing with advanced technology the term "advanced" needs to be defined first. Within the scope of this paper the following areas associated with advanced decoy technology will be addressed:

- Infrared Counter-Countermeasures
  - Rise-time discrimination
  - UV/VIS discrimination
  - Area temperature matching
- Advanced Countermeasure Technology
  - Spectrally adapted payloads
  - Liquid pyrophorics
  - Enhanced performance of black body compositions
  - Kinematic flares
  - Miscellaneous technologies
- Operational Advanced Infrared Countermeasure Munitions

Figure 1 displays the necessary information to evaluate targets.

## 2 Infrared Counter-Countermeasures

After deployment of first generation missiles, AAMs and SAMs (see Table 1), one soon became aware of an IRCM capability such as the widely distributed MTV flares. In order to discriminate against those IRCMs, certain fixes were implemented in seeker heads. Table 1 gives missile seeker technology including CAR-, CAT- and FPA-technology and operational examples.

In Ref. [1] the spectral and kinematical discrimination have already been discussed.

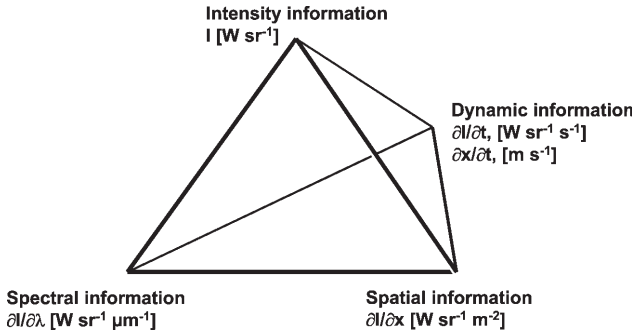


**Figure 1.** Quadruple technology based target selection.

* E-mail: ernst.christian.koch@diehl-bgt-defence.de

**Table 1.** Missile technology

| Generation | Signal modulation | Remarks | Detector | Operational | Reference |
|---|---|---|---|---|---|
| 1st | Reticle | Spin scan, Amplitude modulation | Mono-color IR | SA-7, SA-9, SA-13, AIM-9B | [90] |
| 2nd | Reticle | Con Scan, Frequency modulation | Mono-color IR | SA-14, SA-16, AA-8, AIM-9L/M | [1, 90] |
| 3rd | Rosette Scanning | Conical scan | UV/IR | FIM 92 B/C, SA-18 | [90] |
| 3rd | Cross Array Tracker | Conical scan | Mono-color/ Two color | AA-11 | [90, 91] |
| 3rd | Concentric Annular Ring Tracker | Con Scan | Mono-color | AA-10 | [90, 92] |
| 4th | Focal Plane Array | | Mono-color IR | IRIS-T | [15] |
| 5th | Focal Plane Array | | Hyper-spectral | none yet | |

### 2.1 Rise-Time Discrimination

When flares are deployed as reactive IRCM, the fast spatial separation between flare and platform requires that the flare rapidly attains its maximum radiant intensity before it leaves the field-of-view (FOV) of the seeker [3]. The fast ignition now causes a radiation spike whose intensity may be an order of magnitude higher than the plateau intensity [4, 5]. Both the fast rise as well as the potential steep decline of intensity, after ignition has been achieved, may give rise to discrimination by a seeker head.

One way to overcome this discrimination can be witnessed with many Russian aerial platforms such as e.g. SU 22 or MIG 29. Designers have adopted flare dispensers in up- and forward direction in order to allow for longer residence of the flare within the FOV as can be witnessed on the MIG 29 pictures in Ref. [6] (see Figure 2). It is obvious, that the rise-time for such a deployment may be less steep as can also be seen from the specification of a British substitute for the MIG 29 flare which calls for a rise-time of no less than 1.4 s to attain a peak intensity of 2.5 kW $sr^{-1}$ in the 3 – 5 μm range [7].

### 2.2 UV/VIS Discrimination

The Stinger POST (Passive Optical Seeker Technique) comprises a dual mode seeker similar to the one described in a disclosure by Walker [8]. It is based on a co-focal arrangement of UV-sensitive cadmium sulfide (CdS) (0.3 – 0.5 μm) [9, 100] and an IR detector, which is unspecified but most likely, is a cooled photoconductor of indium antimonide (InSb). After modulation of background and target signature, the dual mode detector yields signals proportional to the incident radiation in both IR and UV. A true aerial target exhibits a positive contrast in the IR with respect to the background, but a negative contrast in the UV. In the case of Mg-based flares, in addition to their strong positive IR contrast, the inherent UV emission [10] also causes a positive contrast, which is not typical of a true target thus allowing discrimination. Likewise the sun, as it may appear in the FOV, is rejected by its strong positive UV contrast [11].

Grundler has proposed to protect aircrafts by attaching UV sources – such as Hg-lamps – to the airframe in order to provide the platform with a false UV signature that may give rise to discrimination by UV/IR guided missiles [12].

### 2.3 Area Temperature Matching

With the invention of imaging seeker heads applying focal plane arrays (FPA) a temperature map of the target is easily constructed. Depending on the type of detector material the FPA may be able to distinguish between the plume, engine and cooler parts of an aircraft. Thus the missile in the endgame may home on these cooler and more vulnerable parts such as the canopy in order to achieve a higher lethality upon impact [13] as it has been reported for the Russian missile AA 11 [14]. In addition the number of pixels illuminated must rise with $r^{-2}$ as the distance between missile and target $r$ becomes smaller whereas the corresponding number of pixels of a spot flare does not increase likewise. Figure 2 gives 3 – 5 μm image of a MIG 29 plane by an FPA seeker taken from Ref. [15] and a visual picture of a similar scene taken from Ref. [6]. Resolution of the seeker allows for detection of the airframe with canopy, tail, pipes and plume. Above in the picture are the trails of two IR flares, imitating the propulsion unit quite well.

## 3 Advanced Countermeasure Technology

### 3.1 Spectrally Adapted Payloads

The main activities in flare development today are devoted to spectral adaptation. The infrared (IR) signature of an aerial platform such as a jet plane is mainly determined by the selective emissions of the hot plume. Figure 3 shows the spectrum of a kerosene plume [16] and a MTV flare in the 2 – 5 μm range [17]. The vertical lines show ranges for both α- and β-band, which have been chosen to coincide with the atmospheric transmission windows [18].

Whereas the color ratio $\theta_{\alpha/\beta}$ for the MTV flare is ~ 1.3 the kerosene plume yields a color ratio of $\theta_{\omega/\beta} < 0.5$.

Generally there are two ways to achieve spectral adaptation.

 

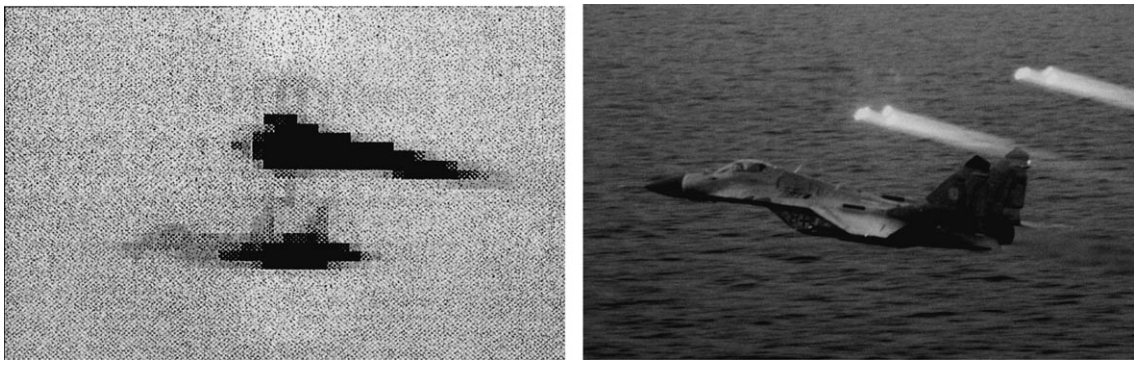

**Figure 2.** FPA image and visual image of MIG 29 expelling flares taken from Ref. [6, 15].

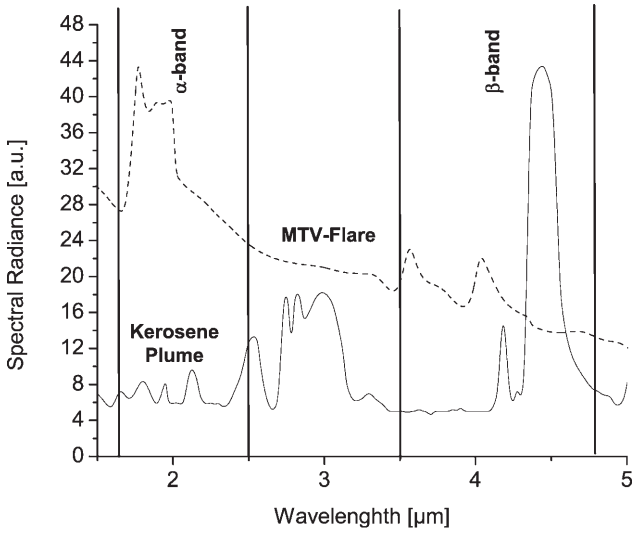


**Figure 3.** Spectrum of kerosene plume [16] and MTV flare [17] in 2 – 5 µm range.

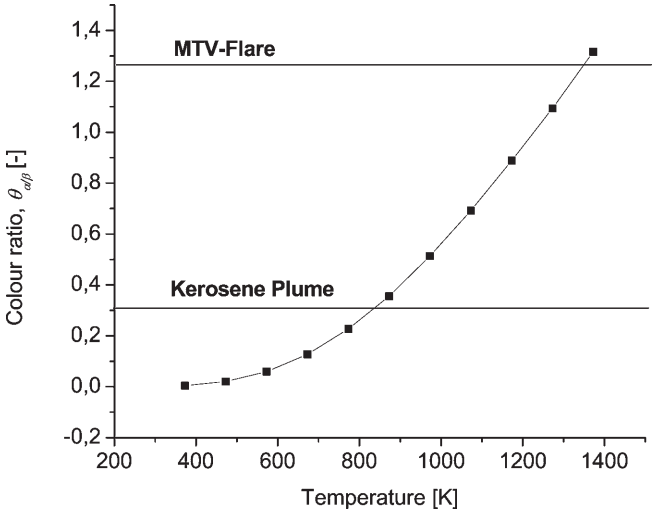


**Figure 4.** Color ratio $\theta_{\alpha/\beta}$ for a black body as a function of temperature.

The first approach is to use compositions that upon combustion emit predominantly in the 4 – 5 µm range and show only minor emission in the 2 – 3 µm range.

The second approach can be derived directly from the laws of radiation. As Wien's displacement law teaches us the emission maximum of a black body or grey body radiator is shifted to shorter wavelength with rising temperature. Figure 4 shows the intensity ratio for both α- and β-band as a function of temperature. It is obvious that only a body having a temperature of less then 900 K will provide a color ratio $\theta_{\alpha/\beta}$ smaller than 0.8.

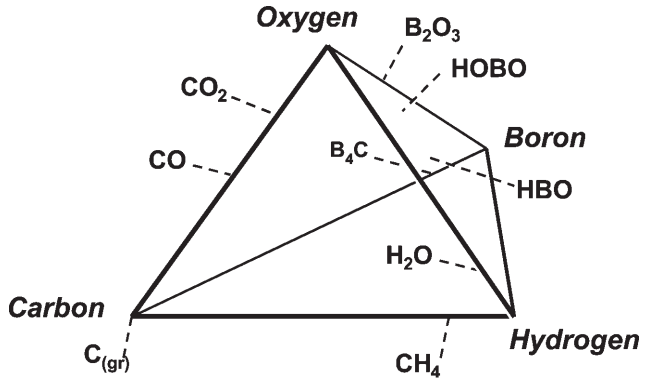


**Figure 5.** Quaternary C–H–B–O diagram with wanted and unwanted emitters

### *3.1.1 Selectively Emitting Compositions*

There are only a few elements that make up the building blocks of suitable species to emit selectively in the 3 – 5 µm band. These elements are carbon, boron, oxygen and hydrogen. Figure 5 shows the quaternary diagram giving position of the favorable (CO, $CO_2$, HBO, $B_2O_2$, $B_2O_3$, HO-B=O, $B_4C$) and unfavorable ($C_{(gr)}$, $H_2O$, $CH_4$) emitters. Naturally there are a lot more unfavorable emitters like e.g. HF, etc. which will not be discussed here (see Table 2 for spectral details).

Table 2 lists the predominant wavelengths and band strength of certain favorable and unfavorable emitters. The most important emitter in the 3 – 5 µm range thus is $CO_2$

 

**Table 2.** Selective emitters [25, 46]

| Emitter | Wavelength [μm] | Band Strength at 300 K [$cm^{-2} \cdot atm^{-1}$] | Reference |
|---|---|---|---|
| CO | 4.67 | 250.36 | [113] |
| | 2.35 | 1.97 | [113] |
| | 1.57 | 0.011 | [93] |
| $CO_2$ | 2.0 | 1.6 | [93] |
| | 2.7 | 67 | [93] |
| | 4.3 | 2700 | [93] |
| | 4.9 | 0.6 | [93] |
| $H_2O$ | 1.14 | 1 | [93] |
| | 1.38 | 18 | [93] |
| | 1.87 | 24 | [93] |
| | 2.7 | 220 | [93] |
| | 6.3 | 300 | [93] |
| $CH_4$ | 2.37 | n.a. | [94] |
| | 3.31 | 290 | [95] |
| NO | 5.33 | 132 | [93] |
| | 2.69 | 2.2 | [93] |
| | 1.80 | 0.044 | [93] |
| HCl | 3.47 | 155 | [113] |
| | 1.77 | 3.52 | [113] |
| HF | 2.53 | 389 | [113] |
| | 1.29 | 12.30 | [113] |
| $B_4C$ | 1 | 1 [$cm^2 \cdot g^{-1}$] | [96] |
| | 2 | 6 [$cm^2 \cdot g^{-1}$] | [96] |
| | 3 | 10 [$cm^2 \cdot g^{-1}$] | [96] |
| | 4 | 10 [$cm^2 \cdot g^{-1}$] | [96] |
| | 5 | 100 [$cm^2 \cdot g^{-1}$] | [96] |
| HO−B=O | 4.94 | 1375 | [115] |
| | 2.72 | 650 | [115] |
| F−B=O | 5.00 | 1760 | [115] |
| HBO | 4.45 | ~1000 | [115] |
| $B_2O_3$ | 4.83 | w | [26] |
| | 4.98 | s | [26] |
| $B_2O_2$ | 5.11 | s | [26] |
| | 4.74 | vw | [26] |
| M-$BO_2$ M=Li, Na, K, Cs | $^{10}$B: 4.84/ $^{11}$B: 5.01 | vw | [27a] |

which is by a factor of ~10 more intense than both CO and $H_2O$.

In this context Posson has mentioned that it is important to take care of a low $H_2O$ content of the combustion products, since too much $H_2O$ emission will deteriorate the spectral color ratio $\theta_{\alpha/\beta}$ [19]. Webb and van Rooijen confirmed this on the basis of their calculations. They investigated the color ratio of hypothetical combustion plumes as a function of temperature, CO−$CO_2$−$H_2O$ ratio and soot content [20].

Aside from the $H_2O/CO_2$ ratio, the color ratio $\theta_{\alpha/\beta}$ is most strongly influenced from the volumetric amount of soot present in the flame. So at soot - volume fractions larger than $10^{-8}$ [$m^3 \cdot m^{-3}$] the color ratio becomes larger than 0.8 and thus is no longer acceptable.

The compositions will be treated as a function of the element responsible for selective emission.

#### 3.1.1.1 Compositions Based on Carbon

As mentioned in Ref. [1] Ase and Snelson have been the first to recognize the paramount importance of $CO_2$ and CO as selectively emitting entities as well as the relative C/H ratio in determining the spectral ratio $\theta_{\alpha/\beta}$ in spectrally adapted flare compositions [21]. Additionally they pointed out the unfavorable influence of soot towards the color ratio.

In general CO and $CO_2$ generation can be achieved by stoichiometrically adjusted compositions containing virtually any carbon source and any oxidizer. Nevertheless the C/O ratio of the carbon source or the bulk composition also plays an important role, as it determines the amount of $CO_2$ available in the primary reaction zone. Thus too high carbon loads may lead to "sooting" flames.

The first composition to rely completely on $CO_2$ emission, by coincidence, was shown by Nielson in his disclosure on propelled black body flare payloads [22]. It was not his intent to develop a color adapted flare composition. Rather, his objective was to produce gasses for thrust. He presents an IR spectrum for HTPB/ammonium perchlorate/magnesium mixture. Although high in hydrogen due to both AP and HTPB, the composition gives an appropriate color adapted ratio. Nevertheless a quick look at the radiant intensity scale of the computed spectrum (see Figure 10) shows the major drawback of this composition as compared to compositions No. 2–5, that is an unacceptably low specific radiant intensity. Finally the magnesium will certainly rule out any operational application since the strong UV emission feature [10] would cause rejection by two-color seekers such as mentioned above.

Composition No. 1

- Magnesium 22 wt-%
- AP 63 wt-%
- HTPB 15 wt-%

Callaway has offered a simple solution to spectral adaptation by proposing common whistle compositions for use in spectrally adapted payloads [23]. These compositions are based on potassium perchlorate ($KClO_4$) and potassium benzoate ($C_6H_5CO_2K$) with either Viton®, cyclic nitramines (RDX) or aromatic nitro-compounds (HNS) as binders. A typical composition is given below:

Composition No. 2a/b

- Potassium benzoate 30 wt-%, particle size < 60 μm
- Potassium perchlorate 65 wt-%, particle size < 60 μm
- Binder 5 wt-% (either Viton®, or RDX)

The combustion of binder-free whistle system potassium perchlorate/potassium benzoate has recently been studied by Charsley and co-workers [24]. They investigated burn rate, exothermicity and released gas volume as a function of the stoichiometry. Figure 6 gives combustion temperature calculated with NASA CEA [25] and burn rate from Ref. [24] as a function of stoichiometry. As the maxima of both plots coincide it is obvious that the burn rate is mainly a function of the combustion temperature. The evolved gas volume is also very important since it relates directly to the size of the radiating area. This has been compared (see Figure 7) with calculated molar fraction of gaseous products

 

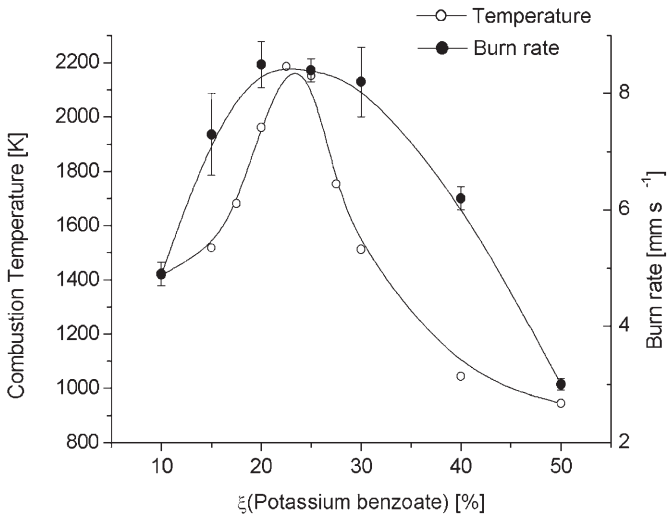


**Figure 6.** Comparison of measured burn rate [24] and calculated combustion temperature [25].

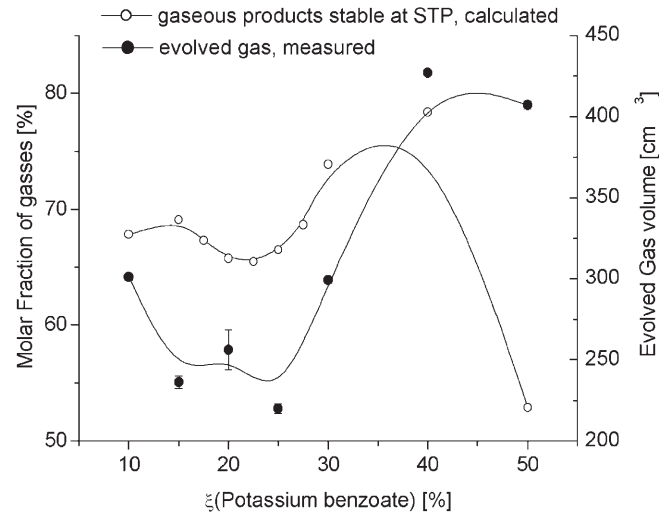


**Figure 7.** Comparison of measured gas evolution [24] and molar fraction of gaseous products [25].

stable at STP. Despite deviations at $\xi_{(Benzoate)} > 0.4$ the plots are comparable in shape. The gas volume now is minimum with highest burn rate but increases with increasing benzoate content. So at the chosen stoichiometry, (comp. No. 2a/b) ($\xi_{(Benzoate)}$: 0.3) both burn rate and released gas volume are high. In addition, the proposed application of nitramines as binders should enhance the combustion rate and due to their high amount of nitrogen release, a further increase in luminous radiating surface area results.

Although Callaway proposes also to use fuels such as sucrose ($C_{12}H_{22}O_{11}$), lactose ($C_{12}H_{22}O_{11}$), or starch ($(C_6H_{10}O_5)_n$, it is known that these are highly oxidized and hence will give only low combustion enthalpy. In addition the high hydrogen content may be detrimental with respect to the color ratio.

Posson recently has devoted a large piece of work to the spectral adaptation problem and addressed the problem of the "right" $H_2O/CO_2$ ratio [19]. Posson proposes a series of carbon rich and hydrogen-lean fuels such as e.g.

- Aromatic polycarboxylic anhydrides, such as mellitic acid trianhydride $C_6(C_2O_3)_3$, benzene tetracarboxylic dianhydride, $C_6H_2(C_2O_3)_2$ and/or benzophenone tetracarboxylic dianhydride $(C_6H_3(C_2O_3))_2CO$,
- Lactones and quinones
- Alkyne derivatives

These fuels are blended with potassium perchlorate in proportions ranging

- Fuel 60 – 80 wt-%
- Oxidizer 20 – 30 wt-%
- Binder 2 – 8 wt-%

depending on chosen combustion chemistry (stoichiometric versus afterburning conditions).

Below a spectrally matched composition is given based on Tris-2′,2″,2‴ cyanoethylamine (TCEA), $C_6H_6N_4$.

Composition No. 3

- Potassium perchlorate 77 wt-%
- TCEA 18 wt-%
- Viton® 5 wt-%

The composition was compacted to a density of 1.91 g cm$^{-3}$ and upon combustion it gave a color ratio $\theta_{2-3\ \mu m/3-5\ \mu m} = 0.52$ in still air [19].

Posson also gives the stoichiometry of a suitable ignition composition for spectrally adapted flare compositions:

Ignition Composition for spectrally adapted flares

- PTFE 12 wt-%
- Viton® 12 wt-%
- $KClO_4$ 62 wt-%
- Boron 14 wt-%

According to NASA CEA calculation this composition yields about equal amounts of both CO and FBO, the latter molecule showing broad emission features around 5 μm with a band strength of 1760 cm$^{-2}$ MPa$^{-1}$, comparable to $CO_2$.

Other extrudable igniter compositions for spectrally adapted decoy flares have been disclosed by Nielson and co-workers [106]. These are based on boron/potassium nitrate and a water soluble binder. One such advantageous composition is given below.

Extrudable Ignition Composition for spectrally adapted flares

- $KNO_3$ 78 wt-%, mean particle size: 35 μm
- Boron 15 wt-%, purity 90 – 92 %
- Polyacrylamide 7 wt-%, Cytec Cyanamer N-300™, mol-wt: $1.5 \times 10^7$.
- Water 14.5 wt-% (additive)

 

**Table 3.** Stoichiometry, mass consumption rate, $\dot{m}$, and specific intensity, $E_\lambda$, according to Ref. [102]

| Mg [wt-%] | $Sr(NO_3)_2$ [wt-%] | Binder [wt-%] | $\dot{m}$ [g $s^{-1}$ $cm^{-2}$] | $E_{2-2,4\,\mu m}$ [J $g^{-1}$ $sr^{-1}$] | $E_{3-5\,\mu m}$ [J $g^{-1}$ $sr^{-1}$] |
|---|---|---|---|---|---|
| 18 | 72 | 10 | 0.39 | 7.6 | 73 |
| 27 | 63 | 10 | 0.53 | 12.5 | 102 |
| 36 | 54 | 10 | 0.95 | 14.9 | 123 |
| 45 | 45 | 10 | 1.03 | 21.5 | 136 |
| 54 | 36 | 10 | 0.95 | 22 | 140 |
| 63 | 27 | 10 | 0.78 | 16.4 | 133 |

The compositions may also include up to 2 wt-% of fibers made from combustible polymers to enhance the mechanical strength of the igniter material.

Mujumdar has investigated the radiant intensity of a series of compositions based on magnesium, strontium nitrate, $Sr(NO_3)_2$, and polyester resin ($C_{14}H_{18}O_7$) [102]. Among the stoichiometries investigated $Mg/Sr(NO_2)_3$/binder 45/45/10 provides the highest specific intensity and highest burn rate in the system. Table 3 lists stoichiometry, specific intensity and mass consumption rate.

The author has developed spectrally balanced compositions based on olefinic and aromatic cyanocarbons as fuels [104]. Suitable cyanocarbons are e.g. tetracyanoethylene $C_2(CN)_4$ and 2,4,6-tricyano-1,3,5-triazine, $C_3N_3(CN)_3$, Cyanil, $C_6(O)_2(CN)_4$ etc. Cyanocarbons in contrary to lactones and carboxyanhydrides and carboxylates as claimed by Callaway [23] and Posson [19] due to their high positive enthalpy of formation allow much higher combustion rates, flame temperatures and thus higher pointance values.

#### 3.1.1.2 Compositions Based on Boron

Boron provides a series of beneficial emitters such as $B_2O_2$, $B_2O_3$, FBO, HBO, HOBO and gaseous alkali metaborates ($MBO_{2(g)}$) (see Table 2) [26, 27a, 107, 115] all mainly based on the B = O vibration mode. In addition to that boron is a highly energetic fuel and helps to enhance the combustion speed of a pyrolant.

An early attempt on a boron based spectrally adapted composition had been reviewed in Ref [1]. It is the composition by Herbage and Salvesen [28]. This composition is a blend of MTV, aluminum, boron, hexamine, potassium nitrate and ammonium perchlorate.

Composition No. 4

- Magnesium 10.150 wt-%
- Aluminium 9.900 wt-%
- Boron 4.125 wt-%
- Urotropine 8.250 wt-%
- Ammonium perchlorate 42.075 wt-%
- Potassium nitrate 6.600 wt-%
- PTFE 4.900 wt-%
- Viton® 14.000 wt-%

It is virtually impossible to give a detailed combustion mechanism for such a complex system. Nevertheless primary reactions between Mg and fluorocarbon entities are quite likely. The resultant soot is oxidized by the AP to give $CO_2$. Boron reacts with both fluorocarbons and potassium nitrate to give $KBO_2$ and FBO.

Smit and co-workers investigated the spectral features of boron/lithium nitrate and boron/sodium nitrate pyrolant combustion [26]. They identified only borate species emitting close to 5 μm.

Callaway in his disclosure on spectral flares [23] also mentions boron/potassium nitrate/Viton® and boron/silicon/potassium nitrate/Viton® compositions.

Composition No. 5

- Potassium nitrate 70 wt-%
- Boron 30 wt-%
- Viton® 5 wt-%

Barnes and co-workers investigated the thermochemistry and combustion behavior of boron/potassium nitrate pyrolants [29]. The combustion temperature does not correlate with the burn rate as it is the case with many metal/metalloid/oxidizer systems [17]. So the maximum burn rate occurs at $\xi_{(Boron)} = 0.5$ (Figure 8). The amount of calculated gaseous products nicely matches with the experimentally determined values for evolved gas. The main emitter $KBO_{2(g)}$ has its highest concentration at $\xi_{(Boron)} = 0.125$ (Figure 9). At the proposed stoichiometry of $\xi(Boron) = 0.3$ in Callaway's disclosure [23], significant amounts of condensed BN (20 %) are present which will deteriorate the color ratio.

#### 3.1.1.3 Computed Composition and Spectra

The molar fractions for CO, $CO_2$, $CH_4$, $H_2O$, $O_2$, $N_2$ and soot for the compositions No. 1 – No. 4 have been calculated

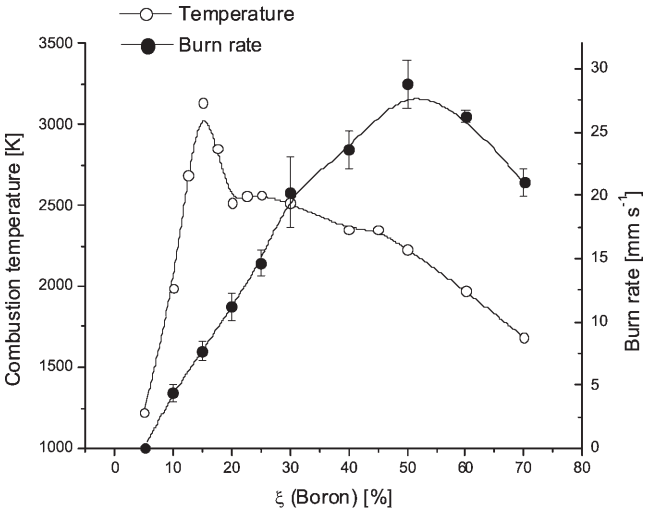


**Figure 8.** Comparison of measured burn rate [29] and calculated combustion temperature [25].

 

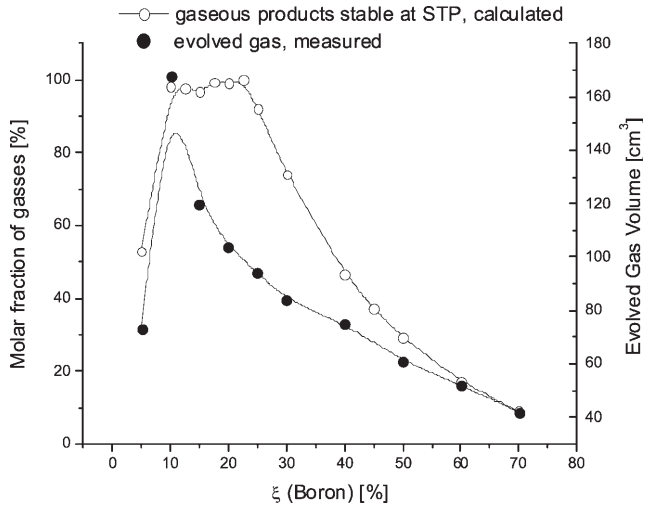


**Figure 9.** Comparison of measured gas evolution [29] and molar fraction of gaseous products [25].

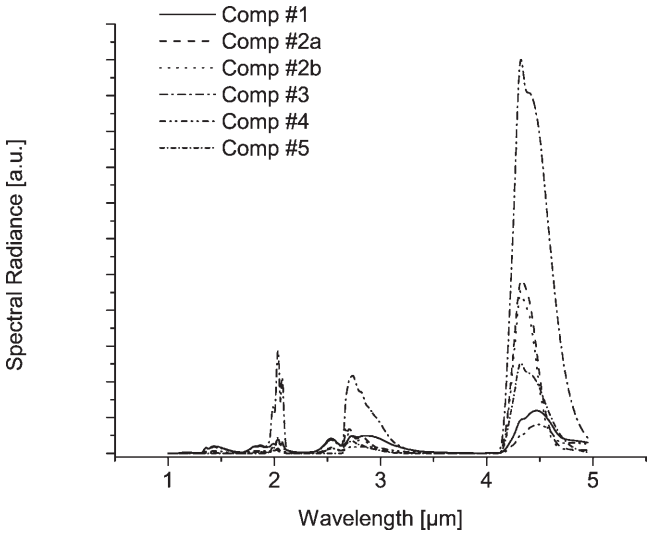


**Figure 10.** Computed spectra [30] of spectrally matched compositions

for the adiabatic case [25] and are listed in Table 4. All compositions are substantially free of particulate carbon. Nevertheless significant amounts of condensed potassium species such as $K_2CO_{3(l)}$ and $KF_{(l)}$ occur (not shown here). The benzoate-type compositions No. 2a/b show the highest CO content whereas composition No. 3 has the highest $CO_2$ content and the second highest combustion temperature after composition No. 1.

The molar fractions of these constituents were used as input for the RADCAL narrow band model [30]. From the calculation it follows that composition No. 1 is the least in intensity whereas composition No. 3 is the best (Figure 10).

Cliff recently investigated spectral characteristics of flare compositions based on alkali dinitramides NaDN and KDN as potential oxidizers in boron/HTPB based IR-decoy flare formulations [31]. However he gave no information on burn rate and absolute intensity.

**Table 4.** Molar fractions of compositions No. 1 – 5 according to Ref. [25]

| Comp | T [K] | CO | $CO_2$ | $H_2O$ | $CH_4$ | $N_2$ | $O_2$ | Soot | Binder |
|---|---|---|---|---|---|---|---|---|---|
| 1 | 2752 | 21.76 | 1.61 | 12.72 | 0.00 | 6.40 | 0.00 | 0.00 | HTPB |
| 2a | 1480 | 32.77 | 22.02 | 12.60 | 0.00 | 2.76 | 0.00 | 0.00 | RDX |
| 2b | 1433 | 36.80 | 20.07 | 11.02 | 0.00 | 0.00 | 0.00 | 0.00 | Viton® |
| 3 | 2702 | 11.72 | 25.80 | 11.89 | 0.00 | 10.45 | 4.76 | 0.00 | Viton® |
| 4 | 2576 | 23.22 | 0.08 | 0.50 | 0.00 | 9.30 | 0.00 | 0.00 | Viton® |
| 5 | 2559 | 5.00 | 0.00 | 0.00 | 0.00 | 0.00 | 0.00 | 0.00 | Viton® |

#### 3.1.1.4 Compositions Based on Silicon

Ase and Snelson in their paper [21] investigated the radiance of $SiH_4$/air combustion in both 2 – 3 μm and 4 – 5 μm bands. They observed a ratio of $\theta_{4-5\ \mu m/2-3\ \mu m} = 3$ as was observed also with pure CO/air. This is in fact puzzling since silicon oxides in the gaseous state are not known to give any selective emission in the 4 – 5 μm range [32, 33]. The fact that the $SiH_4$/air-flame was "fairly" bright, as described by the authors, indicates the presence of incandescent particles such as e.g. $SiO_{2(s)}$. Silica on the other hand in Ref. [34] has been mentioned to show strong selective emission at 4.4 – 4.9 μm when heated to T ~ 1500 K. In contrast the gaseous species $SiO_{(g)}$ and $SiO_{2(g)}$ display emission at 8.2 and 7.1 μm. In the case of incomplete combustion of the $SiH_4$, there may be significant amounts of $SiH_4$, SiH, $SiH_2$ or $SiH_3$, that may give rise to emission at either 4.6, 4.9, 5.0 or 4.6 μm [27b)] as has been observed by others [35, 36]. In silane flames the formation of $H_2$ has also been observed, thus selective emission from $H_2O$ might not occur. In addition, with low concentration of $SiH_4$, very low combustion temperatures down to 750 K have been measured [35]. As discussed above (see Figure 4) radiating bodies having $T < 900$ K will provide a color ratio $\theta_{\omega/\beta}$ that is still $< 0.8$. In view of this the observations by Ase and Snelson may be understood.

Andreotti for the purpose of long wave infrared (8 – 14 μm) emitting torch type naval decoys proposes organo-silicon compounds such as polydimethylsiloxane, $(-O-Si(CH_3)_2-)_n$ [37]. Andreotti finds selective emission of $SiO_2$ in the 7 – 8 μm range useful to enhance radiant intensity in the 7 – 14 μm range as compared to pure hydrocarbon fuels.

Wooldridge has investigated the radiation behavior of $SiH_4/H_2/O_2/Ar$ flames in the UV range. Thus it becomes evident that in oxygen rich cases, there is emission in the 200 – 320 nm range due to $SiO_{(g)}$ and $Si_{(g)}$ [38].

Despite the combustion behavior of silanes, silicon may be added to spectrally adapted compositions to alter their exothermicity. In this context it is not surprising that Callaway also proposes to use $KNO_3$/B/Si mixtures as spectrally adapted payloads [23].

Composition No. 6

- Potassium nitrate 70 wt-%
- Boron 20 wt-%

 

**Table 5.** Si-H Vibrations of SiHX compounds according to Ref. [27b] in μm

| X= | Fluorine | Chlorine | Bromine | Iodine | |
|---|---|---|---|---|---|
| $HSiX_3$ | 4.32 | 4.43 | 4.47 | 4.47 | |
| $H_2SiX_2$ | 4.44 | 4.47 | 4.51 | | |
| | 4.45 | 4.50 | 4.54 | – | |
| $H_3SiX$ | 4.54 | 4.54 | 4.54 | 4.56 | |
| $H_4Si$ | | | | | 4.57 |

- Silicon 10 wt-%
- Viton® 5 wt-% (additive)

Besides the above mentioned species $SiH_{(n-m)}X_m$ ($n = 4$, $m \leq 3$) and (X = F, Cl) species have been reported to emit selectively in the 4 μm range (Table 5). In view of formulations containing Si and fluorinated hydrocarbons such as Viton® the formation of such species is also quite likely. Unfortunately the band strengths of these compounds are not known.

The radiative properties of burning polydimethylsiloxanes (PDMS), $[(CH_3)_3Si{-}O[{-}Si(CH_3)_2{-}O]_n\text{-}Si(CH_3)_3]$, with n = average chain length, have been investigated by Hamins et al. [108, 109].

#### 3.1.1.5 Compositions Based on Aluminum

Herbage described a spectrally adapted payload based on aluminum and boron that has been described in Section 3.1.1.2 of this paper. In this context it is noteworthy to mention that several researches assert the beneficial properties of aluminum on the color ratio [101]. This effect is not related to inherent spectral emission properties of aluminum species. Vanpee and co-workers investigated the infrared spectra of trimethylaluminum/oxygen flames. They found that the higher relative radiant intensity, as compared to pure hydrocarbon, is mainly based on the higher exothermicity of the combustion reaction [39]. Thus addition of aluminum to spectral compositions provides increased exothermicity of compositions leading to higher combustion rates and probably enhancement of carbon oxidation kinetics. Hence it is not surprising that Shortridge observed also an improved color ratio in Cast Cured Spectrally Balanced compositions (CCSB) upon addition of ALEX [40, 101].

These CCSB compositions are based on glycidyl azide polymer (GAP) and hexamethylene diisocyanate curative. As oxidizers these compositions are reported to comprise nitrates, probably $NaNO_3/KNO_3$ and/or either oxides probably such light weight, high oxygen materials like $Li_2O_2$, $MgO_2$, $CaO_2$. The fuels of CCSB have not been released.

#### 3.1.1.6 Wind-Stream Degradation of Spectrally Adapted Compositions

Although a composition may give good results under static conditions, that is measurement in still air, application under dynamic conditions, that are wind speeds greater than 25 m $s^{-1}$ [114] and up to Mach 1, drastically reduce performance in terms of both intensity and band ratio. Wind-stream degradation is infiltration of cold air into the flame. This leads to cooling of the flame and thus altered combustion chemistry affecting spectral radiant intensity and distribution.

Although MTV payloads suffer from wind-stream degradation, their starting intensities are much higher as compared to spectrally adapted payloads. Hence wind-stream degradation of spectrally matched compositions is of even higher concern.

Davies and Holley have investigated several unspecified spectrally matched compositions under different wind speeds [41] and observed a decline in intensity in the 4 – 5 μm band by a factor of 7 going from static conditions to about 250 kts = 130 m $s^{-1}$.

Non-optimized boron based compositions - ($B/KNO_3$/HTPB) - show reduction in radiant intensity in the 4 – 5 μm band by a factor of 6.5 for a wind speed of 150 kts (~ 77 m $s^{-1}$). Likewise the ratio 2 – 3 μm/4 – 5 μm increases by a factor of 1.2 when compositions are burned at 150 kts compared to static conditions. This is due to accelerated condensation of the main emitter potassium metaborate, $KBO_2$ which will precipitate out of the gas phase already at T ~ 1400 °C.

### *3.1.2 Temperature Dependent Emitters*

As discussed above, a radiator of suitable temperature also provides the appropriate spectral color ratio. Admittedly the specific intensity will be lower than with the special emitters discussed under Section 3.1.1. Nevertheless a large number of hot bodies will compensate for this disadvantage in low specific intensity. In this context there have been two principles applied so far. The first principle is to use pure solid-state combustion processes, the other is to use low temperature gas phase processes.

#### 3.1.2.1 Solid-State Combustion Emitters

Baldi from Alloy Surfaces developed a process for manufacturing pyrophoric metal foils that provide intense IR radiation upon exposure to air [42]. Depending on the process, these foils instantaneously ignite within a few milliseconds and attain temperatures of up to 1500 °C. Figure 11 gives a sketch of the combustion of pyrophoric foils.

These foils consist of an iron substrate impregnated with a second metal and finally coated with aluminum, which has been rendered porous by a special treatment. Upon contact

 

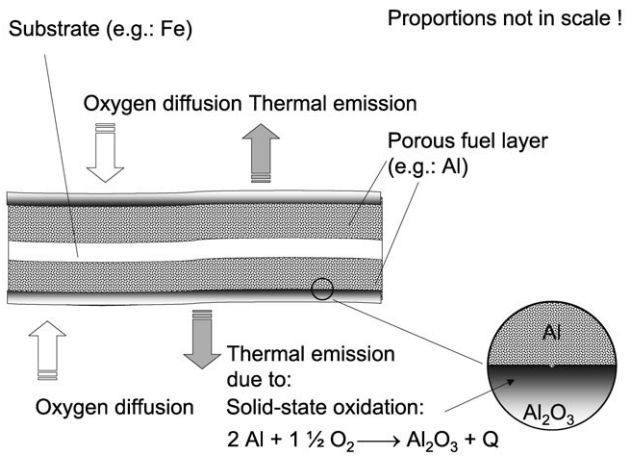


**Figure 11.** Combustion Mechanism of Solid Pyrophoric Agent

with air, the aluminum oxidizes rapidly without any significant emission of visible radiation. Wilharm has given a model for the combustion of porous pyrophoric foils. The combustion performance and thus radiation temperature is mainly dependent on the porosity of the aluminum and on the partial air pressure [43]. Demestihas has simulated the efficiency of AMD/SMD to protect aircraft against reticle based IR seekers [44].

Callaway has proposed to use pyrotechnics constituted from potassium perchlorate and iron consolidated into a disk shape for this purpose [46]. The advantage of this material is the non-pyrophoricity compared to the porous aluminum. Disks such as those proposed indeed find use as heating pellets in thermal batteries since quite a long time [47]. The advantage of those materials is the relatively low luminosity in the visible and the high combustion rate. Nevertheless a severe drawback of the potassium perchlorate/iron system is the need for storage under moist-free, anaerobic conditions in order to prevent instant rusting of the pellets [48]. The burn rate of Fe/$KClO_4$ (14/86) is a function of density and thus may vary between 3 – 12 cm $s^{-1}$ with densities ranging from 2.5 – 5.0 g $cm^{-3}$ [49]. The caloric output is about 1062 J $g^{-1}$ for this stoichiometry [48]. Although the low visible signature of these compositions suits them for covert action applications, the spectral distribution is that of a grey body and thus inappropriate to fight color discriminating seekers.

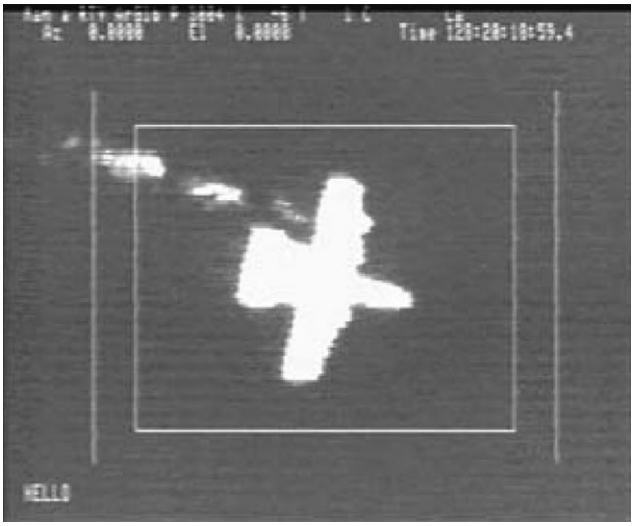

**Figure 12.** FPA image of A 10 Thunderbolt expelling AMD/SMD from COMET dispenser taken from Ref. [45]

#### 3.1.2.2 Low Temperature Gas Phase Combustion

Finally it has been observed that finely dispersed red phosphorus on polymer substrates burns relatively cool to provide a grey body radiation source. Modifying the composition with inert materials such as finely dispersed silica helps to lower the combustion temperature and thus to shift the emission maximum to longer wavelengths within the 4 – 5 μm range [50].

Further lowering of the combustion temperature naturally decreases the radiant output, as is experienced by strong wind-stream degradation of rocket propellant based compositions.

### *3.1.3 Liquid Pyrophoric F*uels

Among the many approaches to provide spectrally adapted plumes, the application of liquid pyrophoric fuels has been investigated in US [16], Canada [116], Sweden [112, 113] and Germany [110] since the early 1970s. Attractive fuels are those that provide short ignition delay and thus reliable ignition under extreme altitude conditions. Ebeoglu has investigated the performance of a series of liquid fuels [16]. The performance parameters are given in Table 6. Among the materials considered - kerosene, trimethylaluminum (TMA), triethylaluminum (TEA), diethylaluminum chloride (DEAC), diethylaluminumhydride (DEAH) and tri-*n*-propylaluminum (TPA) - triethylaluminum displays the most attractive performance.

If we now consider an XMD flare cartridge of the type disclosed in Ref. [51] the payload volume is of the order of ~ 60 $cm^3$. With density of TEA $\rho_{20°}$: 0.837 g $cm^{-3}$ this equals 50.3 g TEA. With $E_{4-5\,\mu m} = 183$ J $g^{-1}$ $sr^{-1}$ [16] we now obtain a total energy of 9.2 kJ. Since operational requirements call for a minimum burning time of 3.5 s, we obtain a peak radiant intensity of $\theta_{4-5\,\mu m} = 2.6$ kW $sr^{-1}$or $\theta_{3.6-4.5\,\mu m} = 4.5$ kW $sr^{-1}$ at 30 kft, that is 9144 m.

The combustion of trimethylaluminum/oxygen mixtures has been investigated by Vanpee [39]. He found that the combustion mechanism of TMA is not very different from pure hydrocarbon combustion. Aluminum only adds to the heat of combustion and thus alters the radiance $M$ [W $cm^{-2}$]. The TMA combustion flame shows distinct Al and AlO lines in both UV and VIS range.

 

**Table 6.** Performance data of kerosene and selected liquid pyrophorics taken from Ref. [16]

| Material | Chemical Constitution | $E_{3.9-5.05\,\mu m}$ [J g$^{-1}$ sr$^{-1}$] | $E_{3.6-4.5\,\mu m}$ [J g$^{-1}$ sr$^{-1}$] | $E_{2.5-3.3\,\mu m}$ [J g$^{-1}$ sr$^{-1}$] |
|---|---|---|---|---|
| Kerosene | $C_{10}H_{22}$–$C_{16}H_{34}$ | 97 | 126 | 94 |
| TMA/TEA | $(CH_3)_3Al/(C_2H_5)_3Al$ | 115 | 278 | 228 |
| DEAC | $(C_2H_5)AlCl$ | 170 | 225 | 147 |
| DEAH/TEA | $(C_2H_5)_2AlH/(C_2H_5)_3Al$ | 174 | 295 | 196 |
| TEA | $(C_2H_5)_3Al$ | 183 | 311 | 237 |
| TPA | $(C_3H_7)_3Al$ | 0.3 | 1.07 | 2.11 |

### 3.2 Enhanced Performance of Black Body Compositions

Although spectral adaptation has the first priority in flare improvement, there obviously still is a need for classical black body payloads. This arises from the fact, that up-to-date spectral payloads can not match the required intensity of black body flares in the 2 – 3 μm band as can be deducted from laws of radiation. Hence it may be beneficial to apply mixtures of several flare types to be on the safe side when it comes to deception of an unknown threat. This doctrine has become known as the cocktail solution [52].

Enhanced black body performance has been the topic of a series of recent disclosures. In general there are two approaches that can be taken:

- Increasing the mass consumption rate with existing compositions
- Using new materials

Whereas increasing the mass consumption rate is more of an interior ballistic design problem, the use of new materials is truly a chemical issue.

#### *3.2.1 Increasing the Mass Consumption Rate*

Tappan has proposed MTV-type flare payloads that are integrated in shallow tubes that allow for discrete combustion instabilities [53]. Since these instabilities cause a distinct dynamic of ambient pressure close to the burning surface, the burn rate is influenced in a way as to be partially doubled thus doubling the mass consumption rate which then causes the radiated energy to double also. Further measures have already been described in Ref. [1].

#### *3.2.2 Optimizing the Radiating Area*

Another approach to alter the radiometric output of a flare is to enhance the radiating surface area $A$ [cm$^2$]. From investigations with visible flares it is known that an optimum light output requires a flare composition with optimum burn rate and diameter in order to have a visible flare plume with optimum optical thickness $\tau$ [cm$^{-1}$] [54]. The total radiant intensity $I_\lambda$ is thus a function of the optical depth $\tau_\lambda$. The latter itself is a function of the physical depth of the flame, $z$, and the linear absorption coefficient of the flame $k_\lambda$.

Nadler [55] and Rosada [56] have independently developed a concept of using segmented payloads that allow for enhanced radiating surface area and optimized optical depth of flames from a single flare. Whereas Rosada relies on a single composition with a different volume-to-surface ratio, Nadler proposes to use at minimum two compositions with different mass consumption rates. A problem in using small flare segments may be their fast consumption leading to a burnout distance that may be insufficient to allow for misguiding an incoming missile. Thus small flare segments should be constituted from relatively slow burning compositions in order to achieve a safe burn-out-distance to the craft.

#### *3.2.3 Using New Materials*

Using new materials can be a stimulus to do research on either fuel or oxidizer side. Thus this section will be divided in new oxidizers and new fuels.

##### 3.2.3.1 New Fuels

Mechanically derived Meta-Stable Alloys

Dreizin recently proposed to use meta-stable alloys synthesized via mechanical cryo-milling of the constituents for energetic materials [57]. In fact these alloys display higher reactivity than common metallic fuels and thus should give rise to higher mass consumption rates. Shortridge reported on the experimental use of these fuels in red and green illuminating flares [58]. This is obviously the unclassified part of the research currently underway.

Mechanically Activated Metal-Oxidizer Mixtures

Dolgoborodov reported on mechanically activated composite material: Al/PTFE [59]. In view of his work, it looks like there is a higher mass consumption rate available after such a mechanical activation of pyrolant mixtures. Nevertheless one should bear in mind that a lower barrier of activation implies a higher sensitivity of these materials.

 

Nano-Sized Metal Powders

Shortridge and Wilharm have reported on the use of nano-sized aluminum powder ALEX® as combustion enhancer in MTV [40, 60, 101]. For MTV type compositions with $\xi(Mg) = 0.54 - 0.55$, the substitution of Mg by ALEX® leads to an increase in burn rate and thus higher performance with a maximum observed at ~27 wt-% ALEX®. Although stoichiometric formulations with $\xi(Mg) = 0.32$ showed enhanced burn rate with ALEX®, the performance was not considered sufficient for application in operational flares. Although ALEX® and other ultra-fine metal powders are known to display very high sensitivity towards electrostatic discharge (ESD), pre-coating the ALEX® with Viton® in a shock-gel process was observed to give compositions relatively insensitive with respect to ESD.

New Organic Fuels in Metal Fluorocarbon Pyrolants

So far, Viton® is the preferred binder in magnesium/Teflon® (MT) type flare materials either for pressing or extrusion process. Viton®, which is (hexafluoropropene vinylidenefluoride copolymer) is high in fluorine and thus adds to the performance in providing fluorinated species. However, it also is very expensive. Another material used in MT type pyrolants is HyTemp®, an acrylate polymer. It is a highly flexible material but does not act as an oxidizer. Its main advantages are the flexibility and the low price. Both materials require the use of solvents such as acetone and hexane both highly flammable and prone to auto-oxidation. In this context a series of fatal explosions have been reported in the last five years, which have been mainly ascribed to peroxide formation while using acetone.

To overcome these problems and perhaps to improve MT pyrolant performance, Nielson has proposed to use aromatic polymers as binders in MT pyrolants that may be processed via extrusion [61]. Nielson showed that pyrolants using polystyrene (PS) and dimethyl phthalate as a binder system provide higher radiant intensity than comparable Viton® based payloads. In addition, the processability of PS is better than that of Viton®. In the following a typical flare composition is given

Composition No. 7

- Magnesium (spherical) 66.0 wt-%
- Teflon® 20.0 wt-%
- Polystyrene 7.0 wt-%
- Dimethyl phthalate 7.0 wt-%.

Such a composition is said to exceed the performance of a Viton® based composition with equal amounts of magnesium and Teflon®.

Nadler, has proposed to use compositions constituted from magnesium, Teflon®, Viton® and graphite [55]. A preferred composition is constituted as follows

Composition No. 8

- Magnesium, gran. 16 63.0 wt-%
- Teflon No. 7 13.5 wt-%
- Viton A 13.5 wt-%
- Graphite 10.0 wt-%

This composition has a burn rate by factor of ~2 higher than a composition based on 54.5% Mg and Teflon®/Viton®. Anyhow from Ref. [62] it is known that the mass consumption rate for MTV (55/40/5) is ~1 g $s^{-1}$ $cm^{-2}$, whereas the mass consumption rate is close to ~2 g $s^{-1}$ $cm^{-2}$ for MTV (63/32/5).

3.2.3.2 New Fluorine-Based Oxidizers

With respect to metal-based pyrolants, the author has investigated a series of new fluorine based oxidizers. Poly(carbon monofluoride) (PMF) better known as graphite fluoride, is a superior oxidizer when compared to poly(tetrafluoroethylene) [63–67]. This stems from the fact, that the enthalpy of formation of graphite fluoride is lower than that of PTFE and that the reactivity of PMF is slightly higher than that of PTFE. With appropriate stoichiometries the performance is by factor of 10 higher than with common MTV. In this context the author investigated the potential of strained fluorocarbons to act as oxidizers in magnesium based pyrolant systems [68–70]. Theoretical investigation of fluorofulleranes as proposed oxidizer call for super burn rate in Mg based pyrolants compared to both PTFE and PMF.

The author has also proposed to synthesize difluoramino substituted graphite $(C(NF_2)_x)_n$ DFSG as oxidizer material. Due to the lower dissociation energy of the N–F bond compared to the C–F bond, the exothermicity of a reaction with halophilic fuels is enhanced. The released nitrogen may either act as flame size expander or react with refractory fuels like Ti and Zr [105].

3.2.3.3 Miscellaneous materials

Gongpei has studied the effect of a series of not less than 18 additives on the radiant intensity of Mg/PTFE (45/55) pyrolant in the 3–5 μm and 8–14 μm band [103]. An unspecified amount of $Fe_3O_4$ added to the baseline composition lead to an increase of radiant intensity in the 3–5 μm band by 50%. An increase in the 8–14 μm band by 100 % was achieved by adding unspecified amounts of Mg/Al alloy.

### 3.3 Kinematic Flares

Since the come in of imaging seekers the trajectory discrimination of targets is an important issue in flare development. A series of designs to overcome trajectory discrimination have been proposed. A general issue with kinematic flares is the need for steering equipment that may

 

pose a danger to other platforms in terms of FOD. Thomas has investigated a series of structural materials for the so-called autophagous design. That is a self-consuming structure by combustion. Thomas advises the use of soft structural materials to reduce risk upon ingestion of decoys and debris by engines. Suitable materials proposed are laminates constituted from plastics and paper type materials combined with layers of energetic materials such as perhaps nitrocellulose [71].

### *3.3.1 Aerodynamic Design*

Upon ejection of a payload under dynamic conditions, the pyrolant block is subjected to a stream of air, which cools down the plume, thus reducing the luminosity. It has been proposed to modify such payloads by inserting a spring actuated aerodynamic front weight that will move out of the payload upon ejection such as to allow for a stabilized flight and to reduce the cooling of the lateral surface. In addition it has been proposed to enhance the combustion plume by shaping the pyrolant grain. Advantageous shapes include:

- holes perpendicular to the length axis of the pyrolant grain at the aft end of the payload
- rocket type nozzle at the aft end of the payload
- shields at the aft end of the payload

These measures allow alteration of the combustion rate and thus help to enhance the plume size [72].

Herbage has designed a flare payload with spring actuated aerodynamic fins and nose [73]. Upon ejection from the flare cartridge the spring-actuated fins deploy and cause the flare payload to orient directly into the wind-stream to attain a reliable trajectory. The nose of the pyrolant payload also contains a weight to stabilize the flare payload. Such weighted noses are found in many new decoys such as e.g. the M 212 spectrally balanced decoy flare [74].

Lecat has devoted a patent to the general structural design of self-righting gliding aerobodies [75].

### *3.3.2 Propelled decoys*

It has been proposed to apply flying decoy bodies with deployable fins that are kinematically adaptable to the platform to be protected. A major drawback of his invention is the large size (l ~ 60 cm, d ~ 10 cm) of the decoy body (folded configuration) making it applicable only from the wing stations and thus reducing armament capacity [76]. Principle designs of such decoy have been described in Ref. [77 – 79]

Smaller propelled decoys, deployable from common flare cartridges, have been proposed for some time.

Brum has proposed to use a decoy-rocket, which subsequently emits SMDs [80].

A composition for propelled decoys, which provides a black body signature, has been proposed by Nielson [22]. One representative composition is given below:

Composition No. 9

- Magnesium 33.00 wt-%
- AP 34.00 wt-%
- Anthracene 15.00 wt-%
- HTPB 14.00 wt-%
- Additives 4.00 wt-%

Although substituting anthracene for PTFE yields a comparable radiant intensity in α– and β-band, the specific thrust is smaller by a factor of 2 for such a composition.

### *3.3.3 Towed Decoys*

Towed radar decoys are applied as countermeasures for some time with considerable success. In view of this, towed infrared decoys should likewise be effective.

At first, towed decoys can overcome the rise-time discrimination [81], since they are attached to the platform and can be ignited in the vicinity of the craft and thus "slowly" increase in intensity to become greater than the platform signature. After the towed decoy has attained the required radiant intensity the distance to the craft is increased in order to provide the necessary miss distance. Since the decoy is connected to the platform, it moves in the same direction as the craft and has the same velocity. Hence kinematic discrimination will not work. Finally the major advantage of towed decoys in general is the fact that one (1) towed decoy could be sufficient to deceive an incoming missile, whereas application of conventional expendables would require expulsion of a series of flares e.g. 4 – 8 flares.

Ref. [82] gives aerodynamic design of a towed flare. Sweeny describes towed decoy for steered expulsion of SMDs [83].

## 3.4 Miscellaneous Technologies

### *3.4.1 Explosive Countermeasure*

For high-speed photography of detonation phenomena the argon bomb is often applied as an illumination source [84]. It is based on the detonative heating of argon gas causing T ~ 20,000 K which leads to complete ionization of argon. The argon plasma emits black body radiation with the peak maximum in dependence of $\lambda_{max} = 2897.9/T$ [μm]. Hence the argon flash has a bluish-white color. Excitation of the surrounding atmosphere causes orange-red emissions, which in total give a pink light. Since the shock wave temperature is also a function of the ionization energy IE [eV], it is obvious that heavier noble gases like e.g. krypton and xenon will allow for higher temperatures and thus allow for higher radiant intensity. The duration of the light emission is proportional to both the detonation velocity and the path-length that the shock wave will travel in the noble gas. So emission may range from a tenth microsecond for small gas layers to a few tens of microseconds for larger gas layers [85].

 

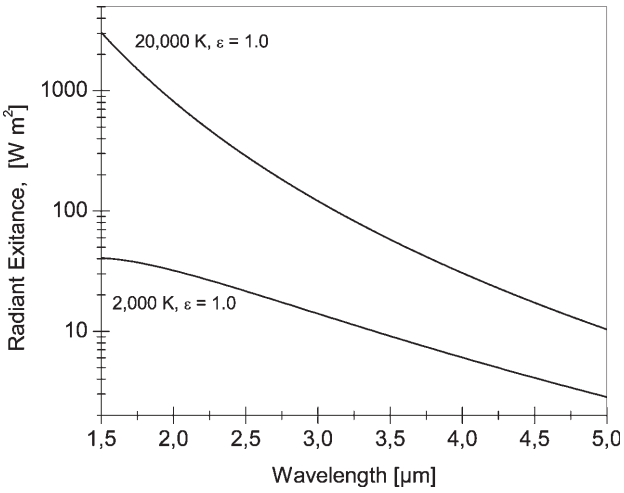


**Figure 13.** Radiant exitance of black bodies having T = 2,000 and 20,000 K

This principle has now been exploited in a patent on explosive countermeasures [86]. The disclosure teaches countermeasure ammunition that consists of an in-situ inflatable balloon transparent to infrared radiation with a centre explosive charge. The balloon is coated with aluminized Mylar®-strips in order to reflect as much as possible radiation towards the seeker. Seeker-head electronics now have automatic gain control that will prevent saturation or damage of a detector. This gain control works on a per millisecond time scale. Whereas conventional pyrotechnic flares may have rise-times in the order of a few tens of milliseconds to reach peak intensity levels, the explosive countermeasure has a rise-time by an order of one magnitude faster than these. Hence the automatic gain control may not work and the seeker detector becomes saturated or eventually damaged causing loss of track.

### *3.4.2 Inflatable Bag Countermeasure*

Since an unshielded pyrolant grain is subjected to rapid cooling upon expulsion in the air, Schwind has proposed to use a bag type countermeasure. This munition consists of an inflatable plastic bag transparent to mid-wave infrared radiation, which is expanded upon ejection from the aircraft by the combustion of a gassy pyrotechnic mixture. The combustion of a secondary composition provides hot particulates radiating in the IR. The bag has a weighted front end with fins in order to orient the flying bag into the air stream. At the aft end of the bag, a vent hole releases the gasses and also furnishes some aerodynamic stabilization [87].

### *3.4.3 Spray Countermeasure for Pyrophorics*

Barbaccia has proposed to gel fuel onboard to give a viscous fuel that can be ignited and expelled into the air to give radiating masses of fuel in the air that may be applied for countermeasure purposes [88].

### *3.4.4 VIS and NIR E*mission

As mentioned earlier, threats and theatres look different today compared to earlier times. In this context great efforts are devoted to accomplish covert action and concealment in military and special operations.

When it comes to covert action and concealment of countermeasure action at least one issue has to be addressed. This is

- Avoidance of excessive radiation of IR countermeasures in inappropriate bands such as VIS and NIR to avoid discrimination by SAMs, visual detection and blinding of night vision goggles (NVG).

To accomplish the latter goal, pyrotechnic payloads must not include metallic fuels known to give intense emissions in either band such as Mg, Ti, Al [10]. In this context the application of aluminum as a fuel in spectrally balanced compositions remains an open issue.

**Table 7.** Operational Advanced Infrared Expendables according to Refs. [74, 97]

| Designation | Calibre [mm] | Payload | Remarks | Platform |
|---|---|---|---|---|
| MJU 27/B | 36 × 148 | SMD | | F 18 |
| MJU 31/B | 52 × 65 | Aerodynamic extendable shroud/MTV | | |
| MJU 35/B | 36 × 206 | SMD | Extended length | F 18 |
| MJU 47/B | 52 × 65 | Propelled Flare | NEW: 390g [98] ASTE | |
| MJU 48/B | 25 × 52 | Hybrid-Payload: MTV/SMD | 60 g MTV, 180 g SMD [98], ASTE | |
| MJU 49/B | 36 × 148 | SMD | | F 18 |
| MJU 50/B | 25 × 25 | SMD | | C-130, A-10, F-16 |
| MJU 51/B | 25 × 52 | SMD | | C-17, C-141, C-51, F-15. F-16 |
| MJU 52/B | BOL | SMD | | F-15 A/B |
| MJU 5188 | 36 × 158 | Liquid pyrophoric | | F-18 |
| MJU 5130 | 36 × 158 | Liquid pyrophoric | | C-130 |
| M 211 | 25 × 25 | SMD | | |
| M 212 | 25 × 52 | Spectrally adapted/ Weighted nose | | |
| DM 69 A2 | 25 × 52 | Red phosphorus | NEW: 180 g [99] | C-130 |

 

## 4 Operational Advanced Infrared Countermeasure Munitions

Table 7 gives information on advanced infrared countermeasure munitions introduced into service by the German Air Force and the United States Air Force.

## 5 Conclusion

The above sheds light on new IRCM developments. It is obvious that upcoming countermeasure developments will become more complex with respect to both chemistry and mechanical design but the countermeasure will largely remain a flare. Some directed energy countermeasures are now close to maturity but will not substitute but act complementary to flares.

The reason for this is quite simple and is already answered in an early book treating IRCM *(...) It may be asked, why flares? (...) the prime among them was the immediate need for a simple and inexpensive source which could operate reliably in a variety of severe environments(...)*[89]. This performance is still to be topped by DIRCM be it LEL, MEL or HEL technology.

## 6 References


[1] E.-C. Koch, Review on Pyrotechnic Aerial Infrared Decoys, *Propellants, Explos., Pyrotech.* **2001**, *26*, 3.

[2] C. Bolkcom, B. Elias, *Homeland Security: Protecting Airliners from Terrorist Missiles*, Report for Congress, Order Code RL31741, February 12, **2003**.

[3] N. Brune, Expendable Decoys, in: J. S. Accetta, D. L. Shumaker (Eds.), *The Infrared and Electro-Optical Systems Handbook, Vol 7 Countermeasure Systems*, SPIE Optical Engineering Press, Bellingham **1996**, pp. 289 – 321.

[4] R. F. Flagg, An Investigation of the Anomalous Ignition Dip Experienced by IR Flares, *16th Int. Annual Conference of ICT,* Karlsruhe, Germany, July 2 – 5, **1985**, pp. 7 – 1

[5] C. J. Tranchita, K. Jakstas, R. G. Palazzo, J. C. O'Connel, Active Infrared Countermeasures, in: J. S. Accetta, D. L. Shumaker (Eds.), *The Infrared and Electro-Optical Systems Handbook, Vol 7 Countermeasure Systems*, SPIE Optical Engineering Press, Bellingham **1996**, pp. 235- 285.

[6] www.fabulousfulcrums.de/action.html

[7] *Flare 26 mm Mk1 Type 1*, Product Information, Chemring Countermeasures, Salisbury, UK, July 2002, available at: www.chemring.com/PDFs/Flare%2026mm%Mk1%Type%201.pdf

[8] C. G. Walker, *Ultraviolet and Infrared Focal Plane Array*, USH0000101, **1984**, The United States of America as represented by the Secretary of the Army, USA.

[9] United States General Accounting Office, *STINGER POST Air Defense Missile: Potential Production Problems – Panned Improvements*, GAO/C-MASA-83-10, 26. January **1983**.

[10] E. Roth, Y. Plitzko, V. Weiser, W. Eckl, H. Poth, M. Klemenz, Emissionsspektren brennender Metalle, *32nd Int. Annual Conference of ICT*, Karlsruhe, Germany, July 3 – 6, **2001**, pp. 163 – 1.

[11] K.-S. Doo, J.-S. Oh, S.-G. Jahng, H.-K. Hong, J.-S. Choi, D.-S. Seo, Simulation of Target Detection in UV and IR Bands, *Proc. SPIE Acquisition, Tracking and Pointing XIV 4025* **2000**, p. 238.

[12] J. Grundler, *Method for the Protection of Aircrafts against Flying Objects Comprising UV-Homing Heads,* U. S. Patent 5 158 351, **1992**, Buck Werke GmbH & Company, Deutschland.

[13] B. Obkircher, *System for Searching, Detecting and Tracking Flying Target*, U. S. Patent 5 964 432, **1996**, Dornier GmbH, Deutschland.

[14] http://www.bharat-rakshak.com/IAF/Missiles/R-73.html.

[15] R. Meller, Neue Lenkflugkörper Luft-Luft Internationale Rüstungskooperation der Luftwaffe, *Soldat und Technik* **1996**, *5,* 302.

[16] D. B. Ebeoglu, C. W. Martin, *The Infrared Signature of Pyrophorics*, AFATL-TR-74 – 92, Air Force Armament Laboratory, May **1974**.

[17] E.-C. Koch, Metal/Fluorocarbon Pyrolants IV: Thermochemical and Combustion Behaviour of Magnesium/Teflon/Viton (MTV), *Propellants, Explos., Pyrotech.* **2002**, *27*, 340.

[18] D. D. Duncan, Atmospheric Transmission, in: J. S. Accetta, D. L. Shumaker (Eds.), *The Infrared and Electro-Optical Systems Handbook, Vol 2 Atmospheric Propagation of Radiation*, SPIE Optical Engineering Press, Bellingham **1993**, p. 130.

[19] P. L. Posson, A. J. Bagget Jr., *Pyrotechnic Composition and Uses Thereof*, U. S. Patent 6 427 599, **2002**, BAE Systems Integrated Defense Solutions Inc., USA.

[20] R. Webb, M. van Rooijen, Using a Theoretical IR Emission Model to Investigate Trends in Theoretical Color Ratios for IR Decoy Flare Applications, *31st International Pyrotechnics Seminar*, Fort Collins, CO, July 10 – 16, **2004**, p. 575.

[21] P. Ase, A. Snelson, Controlled Infrared Output Flares for IRCM Applications, *22nd International Pyrotechnics Seminar*, Fort Collins, CO, July 15 – 19, **1996**, p. 711.

[22] D. B. Nielson, D. M. Lester, *Blackbody Decoy Flare Compositions for Thrusted Applications and Methods of Use,* U. S. Patent 5 834 680, **1998**, Cordant Technologies Inc., USA.

[23] J. Callaway, T. D. Sutlief, *Infra-Red Emitting Decoy Flare,* U. S. Patent Application 2004/0011235 A1, **2004**, GB.

[24] E. L. Charsley, J. J. Rooney, S. B. Warrington, T. T: Griffiths, T. A. Vine, A Study of the Potassium Benzoate – Potassium Perchlorate Pyrotechnic System, *27th International Pyrotechnics Seminar*, Grand Junction, July 16 – 21, **2000**, p. 381.

[25] S. Gordon, B. J. McBride, *Computer Program for Calculation of Complex Chemical Equilibrium Compositions and Applications I. Analysis*, Report NASA RP-1311, NASA Lewis Research Center, Cleveland, Ohio, **1994**.

[26] K. J. Smit, R. J. Hancox, D. J. Hatt, S. P. Murphy, L. V. De Yong, Infrared-Emitting Species Identified in the Combustion of Boron-Based Pyrotechnic Compositions, *Appl. Spectrosc.* **1997**, *51*, 1400.

[27] J. Weidlein, U. Müller, K. Dehnicke, *Schwingungsfrequenzen I, Hauptgruppenelemente*, Georg Thieme Verlag, Stuttgart **1981**, [27a] p. 138; [27b] pp. 261 – 263.

[28] D. Herbage, S. L. Salvesen, *Spectrally Balanced Infrared Flare Pyrotechnic Composition,* U. S. Patent 5 472 533, **1995**, Alliant Techsystems Inc. USA.

[29] P. Barnes, T. T. Griffiths, E. L. Charsley, J. A. Hider, S. B. Warrington, The Properties of the Boron-Potassium Nitrate Pyrotechnic System, *11th International Pyrotechnics Seminar*, Vail, CO, July 7 – 11, **1986**, p. 27.

[30] W. L. Grosshandler, *RADCAL: A Narrow Band Model for Radiation Calculations in a Combustion Environment*, NIST Technical Note 1402, April **1993**.

[31] M. D. Cliff, J. R. Dawe, Metal Dinitramides: New Novel Oxidants for the Preparation of Boron Based Flare Compositions, *24th International Pyrotechnics Seminar*, Monterey, CA, July 27 – 31, **1998**, p. 789.

[32] K. J. Smit, L. V. De Yong, R. Gray, Time Resolved FTIR-Spectroscopy of Silicon Based Pyrotechnics, *21st International Pyrotechnics Seminar*, Moscow, Sep. 11 – 15, **1995**, p. 838.


 

[33] K. J. Smit, L. V. De Yong, R. Gray, Observation of Infrared Emission Spectra from Silicon Combustion Products, *Chem. Phys. Lett.* **1996**, *254*, 197.
[34] E. Lax, M. Pirani, Temperaturstrahlung fester Körper, in H. Geiger, K. Scheel, (Eds.) *Handbuch der Physik*, Bd. XXI, Verlag von Julius Springer, Berlin, **1929**, 268.
[35] K. Tokuhashi, S. Horiguchi, Y. Urano, S. Kondo, Premixed Disilane – Oxygen – Nitrogen Flames, *Combust. Flame* **1990**, *81*, 317.
[36] S. Koda, O. Fujiwara, Silane Combustion in an Opposed Jet Diffusion Flame, *21st Symposium (International) on Combustion*, **1986**, Munich, Germany, p. 1861.
[37] J. Andreotti, A. Hirschman, *Infrared Decoy Method Using Polydimethylsiloxane,* U. S. Patent 5 343 794, **1994**, The United States as represented by the Secretary of the Navy, USA.
[38] M. S. Wooldridge, S. A. Danczyk, J. Wu, Quantitative Evaluation of Vibrational Excitation of SiO $A^1\Pi$-$X^1\Sigma^+$ Flame Emission from a Silane/Hydrogen/Oxygen/Argon Diffusion Flame, *J. Quant. Spectrosc. Radiat. Transfer* **2000**, *64,* 573.
[39] M. Vanpee, E. C. Hinck, T. F. Seamans, Characteristics of Premixed Trimethylaluminium-Oxygen Flames, *Combust. Flame* **1965**, *9*, 393.
[40] R. Shortridge, C. Wilharm, Improved Infrared Countermeasures with Ultrafine Aluminum, *Aircraft Survivability,* Spring **2003**, 45.
[41] N. Davies, D. Holley, Factors Affecting the Radiometric Output of Infrared Flares, *22nd International Pyrotechnics Seminar*, Fort Collins, CO, USA, 15 – 19 July **1996**, pp. 469.
[42] A. Baldi, *Activated Metal and Method of Preparing,* U. S. Patent 4 895 609, **1990**, Alloy surfaces Company Inc, USA.
[43] C. K. Wilharm, Combustion Model for Pyrophoric Metal Foils, *Propellants, Explos., Pyrotech.* **2003**, *28,* 296.
[44] M. Demestihas, *Simulations to Predict the Countermeasure Effectiveness of Using Pyrophorie Type Packets Deployed from TALD Aircraft*, Master's Thesis Naval Postgraduate School Monterey, California, USA, **1999**. Available from NTIS under http://handle.dtic.mil/100.2/ADA375218
[45] Raytheon COMET Countermeasure Pod, Product information available as pdf at http://www.raytheon.com/products/comet/
[46] J. Callaway, *Expendable Infrared Radiating Means,* GB Patent 2 387 430, **2003**, The Secretary of State for Defence in Her Britannic Majesty's Government of the United Kingdom of Great Britain and Nothern Ireland, Great Britain.
[47] W. H. Collins, *Thermal Battery with Metal-Metal Oxide Heating Composition,* U. S. Patent 4 041 217, **1977**, Catalyst Research Corporation, USA.
[48] R. A. Guidotti, *Development History of Fe/$KClO_4$ Heat Powders at Sandia and related Aging Issues for Thermal Batteries*, Sandia Report SAND2001 – 2191, Sandia National Laboratories, Albuquerque, July **2001**, pp. 41
[49] J. W. Reed, R. R. Walters, R. A. Guidotti, A. K. Jacobsen, Burn Rate Studies with Iron/Potassium Perchlorate Heat Pellets, *35th Int. Power Sources Symposium*, 22 – 25 June, **1992**, IEEE, p. 211.
[50] H. Bannasch, M. Wegscheider, M. Fegg, H. Büsel, *Spektrale Scheinzielanpassung und dazu verwendbare Flaremasse,* WO 95/05572, **1995**, Buck Werke GmbH, Deutschland.
[51] P. Brière, M. St.-Onge, A. Roy, B. Paradis, L. Légaré, *XDM Pyrophoric Countermeasure Flare,* U. S. Patent 5 631 441, **1997**, Her Majesty the Queen in right of Canada, as represented by the Minister of National Defence of Her Majesty's Canadian Government, Canada.
[52] S. I. Erwin, "Smart" Flares Being Designed to Defeat Heat-Seeking Missiles, *National Defense Magazine*, December **2003**, *88,* 14.
[53] R. S. Tappan, R. C. Anderson, D. W. Endicott, *High Intensity Infrared Decoy Flare,* U. S. Patent 5 565 645, **1996**, Thiokol Corporation, USA
[54] B. E. Douda, *Pyrotechnic Flare Spectroscopy – A Radiative Transfer Model*, RDTN No. 266, Naval Ammunition Depot, Crane, Indiana, 1 April **1974**.
[55] M. P. Nadler, *Pyrotechnic Pellet Decoy Method,* U. S. Patent 6 675 716, **2004**, The United States as represented by the Secretary of the Navy, USA.
[56] J.-P. Rosada, P. Rousseau, *Infrarotköderpatrone,* DE 44 47 470 A1, **1996**, Etienne Lacroix – Tous Artifices S. A., France.
[57] E. L. Dreizin, Y. L. Shoshin, R. S: Mudry, Preparation and Characterization of Energetic Al-Mg Mechanical Alloy Powders, *Combust. Flame* **2002**, *128,* 259.
[58] R. G. Shortridge, C. K. Wilharm, E. Dreizin, Elimination of Perchlorate Containing Oxidizers from Red and Green Pyrotechnic Flare Compositions, *31st International Pyrotechnics Seminar*, Fort Collins, July 11 – 16, **2004**, p. 851.
[59] A. Y. Dolgoborodov, M. N. Makhov, A. N. Streletskii, I. V. Kolbanev, M. F. Gogulya, M. A. Brazhinov, V. E. Fortov, Detonation-Like Phenomena in Non-Explosive Oxidizer-Metal Mixtures, *Proc. 31st International Pyrotechnics Seminar*, Fort Collins, July 11 – 16, **2004**, pp. 569.
[60] S. K. Poehlein, R. G. Shortridge, C. K. Wilharm, A Comparative Study of Ultrafine Aluminum, *28th International Pyrotechnics Seminar*, 4 – 9 November **2001**, Adelaide, Australia, pp. 597.
[61] D. B. Nielson, D. M. Lester, *Extrudable Black Body Decoy Flare Compositions,* U. S. Patent 6 432 231, **2002**, Cordant Technologies Inc., USA.
[62] E.-C. Koch, A. Dochnahl, IR Emission Behavior of Magnesium/Teflon/Viton (MTV) Compositions, *Propellants, Explos., Pyrotech.* **2000**, *25,* 37.
[63] E.-C. Koch, Poly(kohlenstoffmonofluorid) ein Extrem Energiereiches Oxidationsmittel, *10. GDCh Vortragstagung – Anorganische Funktionsmaterialien:* 26 – 29. September **2000**, Münster, p. A-62.
[64] E.-C. Koch, Fluoreliminierung aus Graphitfluorid mit Magnesium, *Z. Naturforsch., B: Chem. Sci.* **2001**, *56*, 512.
[65] E.-C. Koch, *Pyrotechnic Compositions for Producing IR-radiation,* U. S. Patent 6 635 130, **2003**, Diehl Munitionssysteme GmbH & Co. KG, Deutschland.
[66] E.-C. Koch, Untersuchung von Magnesium/Graphitfluorid/Viton® Thermochemische Eigenschaften - Strahlungsverhalten – Anwendungen, *Forum Explosivstoffe*, Wehrwissenschaftliches Institut für Werk- Explosiv- und Betriebstoffe (WIWEB) Swisttal Heimerzheim, 11.-12. Oktober **2004**.
[67] E.-C. Koch, Metal Fluorocarbon Pyrolants: VI. Combustion Behaviour and Radiation Properties of Magnesium/Poly(Carbon Monofluoride) Pyrolant, *Propellants, Explos. Pyrotech.* **2005**, *30*, 209.
[68] E.-C. Koch, Theoretical Considerations on the Performance of Various Fluorocarbons as Oxidisers in Pyrolant Systems, *34th Int. Annual Conference of ICT*, Karlsruhe, Germany, June 24 – 27, **2003**, pp. 40 – 1
[69] E.-C. Koch, Metal Fluorocarbon Systems: V. Theoretical Evaluation of the Combustion Performance of Metal/Fluorocarbon Pyrolants based on Strained Fluorocarbons, *Propellants, Explos., Pyrotech.* **2004**, *29*, 9.
[70] E.-C. Koch, *Pyrotechnischer Satz zur Erzeugung von IR - Strahlung und Verfahren zu seiner Herstellung,* DE Patent 103 07 627, **2004**, Diehl Munitionssysteme GmbH & Co. KG, Deutschland.
[71] J. P. Thomas, *Autophagous Design and Material Options for Forward Deployed Aircraft IR Decoys with Reduced Risk of Foreign Object Damage*, NRL/MR/6350-03-8672, Naval Research Laboratory, Washington DC, March 7, **2003**.
[72] A. L. Dunne, J. C. Huber Jr., *Infrared Signature Enhancement Decoy,* U. S. Patent 5 074 216, **1991**, Loral Corporation, USA.
[73] D. W: Herbage, W. H. Heinsohn, *Decoy flare,* U. S. Patent 5 400 712, **1995**, Alliant Techsystems Inc., USA.
[74] M. Shoemaker, Special Materials Decoys (SMD) *Briefing to the Australian AOC*, 11.04.**2000**.

 

[75] R. J. Lecat, *Self-Righting Gliding Aerobody/decoy,* U. S. Patent 5 169 095, **1992**, Grumman Aerospace Corporation, USA.
[76] Anonymous, Kombiniertes Scheinziel für die Luftwaffe, (KSL), *Soldat und Technik* **2000**, *12*, 820.
[77] B. Obkircher, J. Steinwandel, M. Heller, R. Willneff, *Flying Device for IR Flying Target Representation,* U. S. Patent Application 2003/0197332 A1, **2003**, Dornier GmbH, Deutschland.
[78] H. Heinz K Scheerer, *Täuschkörper zum Ablenken von zielsuchenden Lenkflugkörpern,* DE 196 01 165 A1, **1997**, Bodenseewerk Gerätetechnik GmbH, Deutschland.
[79] B. Obkircher, *Scheinziel,* DE 39 05 748 A1, **1993**, Dornier GmbH, Deutschland.
[80] R. D. Brum, *Decoy Utilizing Infrared Special Material,* U. S. Patent 5 915 694, **1999**, USA
[81] N. Wardecki, *Protective Means for Fast Moving Object,* U. S. Patent 5 852 254, **1998**, Buck Chem. Tech. Werke, Deutschland.
[82] R. J. Lecat, *Cable Towed Decoy with Collapsible Fins,* U. S. Patent 5 029 773, **1991**, Grumman Aerospace Corporation, USA.
[83] L. R. Sweeny, *Electronically Configurable Towed Decoy for Dispensing Infrared Emitting Flares,* U. S. Patent 6 055 909, **2000**, Raytheon Company, USA
[84] M. Held, High-Speed Photography, in J. Carleone (Ed.), *Tactical Missile Warheads*, Vol 155 *Progress in Astronautics and Aeronautics*, A. R. Seebass (Ed.), American Institute of Aeronautics and Astronautics, Washington **1993**, p. 609.
[85] R. L. Conger, L. T. Long, J. A. Parks, J. H. Johnson, The Spectrum of the Argon Bomb, *Appl. Opt.,* **1965**, *4*, 273.
[86] N. H. Anderson, E. S. Almasy, *Explosive Countermeasure Device,* U. S. Patent 6 324 955, **2001**, Raytheon Company, USA.
[87] R. G. Schwind, *High Speed Inflating Bag Infrared Countermeasure,* U. S. Patent 5 249 527, **1993**, Westinghouse Electric Corp. USA.
[88] P. L. Barbaccia, *Radiative Countermeasure Method,* U. S. Patent 6 352 031, **2002**, Northrop Grumman Corporation, USA.
[89] J. Sarnow, Infrared Emitters, in: F. B. Pollard, J. H. Arnold (Eds.), *Aerospace Ordnance Handbook*, Prentice-Hall, Englewood Cliffs **1966**, 224.
[90] E. Güven, Electrooptical and Infrared Applications in Defense, *Armed Forces Communications and Electronics Association* (*AFCE) Turkye 2003, 6th Int. Seminar Technology for Effective Defense*, 7 – 8 May **2003**, Ankara, p. 27 – 42.
[91] S.-G. Jahng, H.-K. Hong, J.-S. Choi, S.-H. Han, Reticles – Nutating Systems, in: R. G. Driggers (Ed.), *Encyclopedia of Optical Engineering*, Marcel Dekker Inc. **2003**, p. 2417.
[92] H.-K. Hong, S. G. Jahng, K.-S. Doo J.-S. Choi, S. H. Han, Adaptive Infrared Counter Countermeasure for Two Color Spinning Concentric-Annular-Ring Reticle Seeker, *Opt. Eng.* **2001**, *40,* 1093.
[93] C. B. Ludwig, W. Malkmus, J. E. Reardon, J. A. L. Thomson, *Handbook of Infrared Radiation From Combustion Gases*, NASA SP 3080, National Aeronautics and Space Administration, Washington, **1973**.
[94] A. C. Hottel, A. F. Sarofim, *Radiative Transfer*, McGraw-Hill Book Company, New York **1967**, p. 239 – 240.
[95] S. P. Fuss, O. A. Ezekoye, M. J. Hall, The Absorptance of Infrared Radiation by Methane at Elevated Temperatures, *J. Heat Transfer* **1996**, *118,* 918.
[96] U. Werner, H. Mach, M. König, *Strahlungs- und Mikrowellenmessungen an Gasflammen mit Additiven*, Report R 122/78, ISL, Saint-Louis, 13.10.**1978**.
[97] R. J. Ritchie, Army Advanced Infrared Countermeasure Flares, *Aircraft Survivability*, Spring **2003**, 22.
[98] U. S. Flares, Product Information, Esterline Armtec, Coachella available at: http://www.armtecdefense.com/pdf/U.S._Flares_ProdSht_F.pdf
[99] *Ordnance Identification Guide Afghanistan*, Naval Explosive Ordnance Disposal Technology Division, Indian Head Maryland, USA, available at: https://naveodtechdiv.navsea.navy.mil/ AfghanOIG/PDF-high/09-Pyrotechnic.pdf
[100] P. W. Kruse, L. D. McGlauchin, R. B. McQuistan, *Grundlagen der Infrarottechnik*, Verlag Berliner Union GmbH Stuttgart **1972**, p. 461.
[101] R. G. Shortridge, C. K. Wilharm, Improved Infrared Countermeasures with Ultrafine Aluminum, *AIAA 2004-2063*, *45th AIAA/ASME/ASCE/AHS/ASC Structures, Structural Dynamics & Materials Conference,* 19 – 22 April **2004**, Palm Springs, California.
[102] V. A. Mujumdar, S. Jayaraman, Studies on $Mg-Sr(NO_3)_2$ based Pyrotechnic Compositions for Infrared Flare Application, *24th International Pyrotechnics Seminar*, Monterey, July 27 – 31, **1998**, p. 811.
[103] P. Gongpei, *Jamming Performance of Infrared Bait/Chaff*, NAIC-ID(RS)T-0383-95, National Air Intelligence Center, 17. August **1995**.
[104] E.-C. Koch, *Pyrotechnischer Satz zur Erzeugung von IR-Strahlung,* Patent EP1541539, **2005**, Diehl BGT Defence GmbH & Co. KG, Deutschland.
[105] E.-C. Koch, *Pyrotechnischer Satz,* Patent DE 102004018861, **2005**, Diehl BGT Defence GmbH & Co. KG, Deutschland.
[106] D. B. Nielson, G. K. Lund, R. J. Blau, *Flares Having Igniters Formed from Extrudable Igniter Compositions,* U. S. Patent 6 170 399, **2001**, Cordant Technologies. Inc., USA.
[107] A. Büchler, E. P. Marram, Gaseous Metaborates. II. Infrared Spectra of Alkali Metaborate Vapors, *J. Chem. Phys.* **1963**, *39*, 292.
[108] R. Buch, A. Hamins, K. Konishi, D. Mattingly, T. Kashiwagi, Radiative Emission Fraction of Pool Fires Burning Silicone Fluids, *Combust. Flame* **1997**, *108*, 118.
[109] Y. Sivathanu, A. Hamins, G. Mulholland, T. Kashiwagi, R. Buch, Characterization of Particulate from Fires Burning Silicone Fluids, *J. Heat Transfer* **2001**, *123*, 1093.
[110] K. Menke, personal communication, **2005**.
[111] B. Gelin, *Användning av Pyrofora Material i Motmedelsfacklor*, FOA Rapport C 20471-D1(E4, F9), Oktober **1982**.
[112] B. Gelin, *Pyrofora Alkylaluminium Föreningar i Motmedelsfacklor*, FOA Rapport C 20562-E4, November **1984**.
[113] S. P. Fuss, A. Hamins, Determination of Planck Mean Absorption Coefficient for HBr, HCl and HF, *Trans. ASME* **2002**, *124*, 26.
[114] J. N. Towning, Pyrotechnic Flares: Radiant Intensity and radiance calculations, *14th International Pyrotechnics Seminar*, Jersey, UK, September 18 – 22, **1989**, p. 537.
[115] D. W. Boyer, Shock-Tube Measurements of the Band Strengths of $HBO_2$ and OBF in the Short Wavelength Infrared, *J. Quant. Spectrosc. Radiat. Transfer* **1980**, *24*, 269.
[116] J. L. Halpin, K. D. Foster, *Holder for Flames of Pyrophore-Containing Fuels in High-Speed Air,* U. S. Patent, **1988**, Her majesty the Queen in right of Canada, Canada.

## *Symbols and Abbreviations*

| | |
|---|---|
| $\alpha$ | Alpha band 1.8 – 2.5 [μm] |
| $\beta$ | Beta band 3.5 – 4.8 [μm] |
| $\lambda$ | Wavelength [μm] |
| $\tau$ | Optical thickness, [$cm^{-1}$] |
| $\theta_{\alpha/\beta}$ | Colour ratio [–] |
| $\xi$ | Weight fraction [1/100] |
| $I_\lambda$ | Radiant Intensity [W $sr^{-1}$] |
| $L_\lambda$ | Spectral Radiance [W $sr^{-1}$ $cm^{-2}$ $\mu m^{-1}$] |
| $M$ | Radiant Exitance [W $cm^{-2}$] |
| $E_\lambda$ | Specific intensity [J $g^{-1}$ $sr^{-1}$] |

 

| | |
|---|---|
| $C_{(gr)}$ | Graphite |
| CdS | Cadmium sulfide, UV-VIS-detector material |
| InSb | Indium antimonide, IR-detector material |
| AA | Air-to-Air missile, designation for Russian missiles |
| AAM | Air-to-Air Missile |
| ALEX® | Nanosized Aluminium, trademark of Argonide Nanomaterial Technologies |
| AIM | Aerial Intercept Missile |
| AIRCM | Advanced Infrared Countermeasures |
| AM | Amplitude Modulation |
| AMD | Activated Metal Decoy |
| AP | Ammonium perchlorate, $NH_4ClO_4$ |
| ASTE | Advanced Strategic and Tactical Expendable |
| Atm | Atmosphere = 1.01325 $10^5$ Pa |
| CAR | Concentric Annular Ring Reticle |
| CAT | Cross Array Tracker |
| CCSB | Cast Cured Spectrally Balanced |
| COMET | Infrared Countermeasure Pod, product of Raytheon Company |
| DIRCM | Directed Infrared Countermeasure |
| ESD | Electrostatic Discharge |
| FIM | Man-launched Surface-to-Air Missile |
| FM | Frequency Modulation |
| FOD | Foreign Object Damage |
| FOV | Field of View |
| FPA | Focal Plane Array, imaging detector |
| HEL | High-Energy-Laser |
| HNS | Hexanitrostilbene, $C_{14}H_6N_6O_{12}$ |
| HTPB | Hydroxy-Terminated Polybutadiene |
| IR | Infrared |
| IRCM | Infrared Countermeasure |
| kft | Kilofeet = 304.8 m |
| kts | Knots = 0.5144 m $s^{-1}$ |
| LEL | Low-Energy-Laser |
| MANPADS | Man-Portable-Air-Defense-System |
| MEL | Middle-Energy-Laser |
| MJU | Countermeasure Munition |
| MTV | Magnesium/Teflon®/Viton®, flare composition |
| NEW | Netto Explosive Weight |
| NVG | Night Vision Goggles |
| PDMS | Polydimethylsiloxanes, $[(CH_3)_3Si\text{-}O[\text{-}Si(CH_3)_2\text{-}O]_n\text{-}Si(CH_3)_3]$, whith n = average chain length |
| PTFE | Polytetrafluoroethylene, commercially available as e.g. Teflon® trademark of Dupont |
| RDX | *cyclo*-1,3,5-Trimethylene-2,4,6-trinitramine, hexogen, $C_3H_6N_6O_6$ |
| RSIS | Rosette Scanning Infrared Seeker |
| SA | Surface-to-Air missile, designation for Russian missiles |
| SAM | Surface-to-Air Missile |
| STP | Standard Temperature and Pressure, 298.15 K, 0.1 MPa |
| TMA | Trimethylaluminium, $Al(CH_3)_3$ |
| TEA | Triethylaluminium, Al $(C_2H_5)_3$ |
| SMD | Special Materials Decoy, solid pyrophoric material |
| XMD | Experimental Model Decoy, liquid pyrophoric fuel decoy |

(Received February 3, 2005, modified version November 30, 2005; Ms 2005/001)